Structural Durability of Damaged Metallic Panel Repaired with Composite Patches

LEVON MINNETYAN*
Clarkson University
Potsdam, New York 13699-5710

CHRISTOS C. CHAMIS
National Aeronautics and Space Adminstration
Structures Division
Lewis Research Center
Cleveland, Ohio 44135-3191

ABSTRACT: Structural durability/damage tolerance characteristics of an aluminum tension specimen possessing a short crack and repaired by applying a fiber composite surface patch is investigated via computational simulation. The composite patch is made of graphite/epoxy plies with various layups. An integrated computer code that accounts for all possible failure modes is utilized for the simulation of combined fiber-composite/aluminum structural degradation under loading. Damage initiation, growth, accumulation, and propagation to structural fracture are included in the simulation. Results show the structural degradation stages due to tensile loading and illustrate the use of computational simulation for the investigation of a composite patch repaired cracked metallic panel.

INTRODUCTION

IN RECENT YEARS laminated composite patches have been used for the repair of aging aluminum aircraft with existing or potential fatigue cracks. Design considerations regarding the durability of a patch repaired aluminum panel require an a priori evaluation of damage initiation and propagation mechanisms under expected service loading and hygrothermal environments. In general, the controlling design load is tension perpendicular to the orientation of a crack. However, due to the variability of the load direction, combined shear with tensile

*Dept. Civil and Environmental Engrg., Summer Faculty Fellow, NASA Lewis Research Center. Author to whom correspondence should be addressed.

Reprinted from *Journal of* REINFORCED PLASTICS AND COMPOSITES, *Vol. 16, No. 3/1997*

loading must also be taken into account when evaluating the performance of a composite patch repair. Concerns for safety and survivability of a patch-repaired aluminum panel require a quantification of the structural fracture resistance under loading.

Discussion in the current paper is focussed on a composite patch repaired aluminum panel subject to a primarily tensile loading. Damage initiation, growth, accumulation, and propagation to fracture is simulated. Effect of the length of an existing crack is examined with regard to the damage progression and structural durability under applied loading. The damage initiation load and the structural fracture load are quantified.

Fiber composite patches have tremendous advantages of light weight, high strength, durability, flexibility, and corrosion resistance. The multiplicity of options available in the design of a laminate configuration make composites more capable of fulfilling structural patch repair design requirements. However, for certain designs structural interaction between plies with different fiber orientations and the aluminum panel may adversely affect durability, especially in the presence of combined loading. The computational simulation method presented in this paper is well suited to investigate and identify the effects of structural interactions on damage and fracture propagation under design loads and overloads.

For the purpose of the present study, the following terminology is used to describe the various stages of degradation in the composite structure: (1) *initial defect* refers to an existing crack in the aluminum panel that may be due to material/fabrication defect and/or fatigue loading; (2) *damage initiation* refers to the start of damage induced by loading that the composite patch is helping to carry; (3) *damage growth* is the progression of damage from the location of damage initiation to adjacent regions; (4) *damage accumulation* is the increase in the amount of damage in the damaged region with additional damage modes becoming active; (5) *damage propagation* is the rapid progression of damage to other regions of the specimen; (6) *structural fracture* is the ultimate disintegration or fracture of the specimen into two pieces.

METHODOLOGY

The evaluation of composite-repaired airframe structures requires an assessment of their safety and durability under service loads and possible overload conditions. The ability of designing composite patches with numerous possible fiber orientation patterns, choices of constituent material combinations, tow/ply drops, and hybridizations render a large number of possible design parameters that may be varied for an optimal design. The multiplicity of composite patch design options presents a logistical problem, prolonging the design and certification process and adding to the cost of the final product. It is difficult to evaluate long-term durability of composite-repaired structures due to the complexities in predicting their overall congruity and performance, especially when structural degradation and damage propagation take place. The predictions of damage initiation, damage growth, and propagation to fracture are important in evaluating the load carring capacity, damage tolerance, safety, and reliability of such repairs. Quan-

tification of the structural fracture resistance is also fundamental for evaluating the durability/life of composite repaired structures. The most effective way to obtain this quantification is through integrated computer codes that couple composite mechanics with structural analysis and damage progression modeling.

An important feature of computational simulation is the assessment of damage stability or damage tolerance of a structure under loading. At any stage of damage progression, if there is a high level of structural resistance to damage progression under the service loading, the structure is stable with regard to fracture. The corresponding stage of structural damage is referred to as *stable damage*. On the other hand, if damage progression does not encounter significant structural resistance, it corresponds to an *unstable damage* state. Unstable damage progression is characterized by very large increases in the amount of damage due to small increases in loading; whereas during stable damage progression the amount of increase in damage is consistent with the increase in loading.

Internal damage in composites is often initiated as cracking due to normal tensile stresses transverse to the fiber orientation. Further degradation is in the form of additional cracking, delaminations, and fiber fractures that usually lead to structural fracture. Because of the numerous possibilities with material combinations, composite patch geometry, fiber orientations, and loading conditions, it is essential to have an effective computational capability to predict the behavior of composite repaired structures for any loading, geometry, composite material combinations, and boundary conditions. The predictions of damage initiation, growth, accumulation, and propagation to fracture are important in evaluating the load carrying capacity and reliability of composite structures. Quantification of the structural fracture resistance is also required to evaluate the durability/life of composite repaired structures under various loading and environmental conditions, considering also the fabrication process effects.

The CODSTRAN (COmposite Durability STRuctural ANalysis) computer code [1] has been developed for this purpose. CODSTRAN is an integrated, open-ended, stand alone computer code consisting of three modules: composite mechanics, finite element analysis; and damage progression modeling. The overall evaluation of composite structural durability is carried out in the damage progression module that keeps track of composite degradation for the entire structure. The damage progression module relies on ICAN [2] for composite micromechanics, macromechanics and laminate analysis, and calls a finite element analysis module that uses anisotropic thick shell and three dimensional solid elements, as appropriate, to model laminated composites as well as the repaired metallic panels [3].

CODSTRAN is able to simulate damage initiation, damage growth, and fracture in composites and homogeneous materials under various loading and environmental conditions. CODSTRAN has been used to investigate the effect of composite degradation on structural response [4], composite structures global fracture toughness [5], effect of hygrothermal environment on durability [6], damage progression in composite thin shells subjected to internal pressure [7], progressive fracture of steel pressure vessels [8], and the durability of discontinuously stiffened composite panels under compressive loading [9]. The pur-

pose of this paper is to describe application of CODSTRAN to simulate damage progression in a cracked aluminum panel with a composite surface patch for a design investigation that takes into account damage initiation/propagation mechanisms.

Figure 1 shows a schematic of the computational simulation cycle in CODSTRAN. The ICAN composite mechanics module is called before and after each finite element analysis. Prior to each finite element analysis, the ICAN module assembles the composite properties from the fiber and matrix constituent characteristics and the composite layup. The generalized force-displacement and moment-curvature relations are computed by ICAN as:

$$\begin{Bmatrix} \{N_{cx}\} \\ \{M_{cx}\} \end{Bmatrix} = \begin{bmatrix} [A_{cx}] & [C_{cx}] \\ [C_{cx}] & [D_{cx}] \end{bmatrix} \begin{Bmatrix} \{E_{cxx}\} \\ \{W_{cb}\} \end{Bmatrix} - \begin{Bmatrix} \{N_{CTtX}\} \\ \{M_{CTtS}\} \end{Bmatrix} - \begin{Bmatrix} \{N_{CMtX}\} \\ \{M_{CMtX}\} \end{Bmatrix} \quad (1)$$

Where $\{N_{cx}\}$ are the applied in-plane forces, $\{M_{cx}\}$ are the bending moments, $\{E_{cxx}\}$ are the in-plane strains, $\{W_{cb}\}$ are the out-of-plane curvatures, $\{N_{CTtX}\}$ are the thermal forces, $\{M_{CTtX}\}$ are the thermal moments, $\{N_{CMtX}\}$ are the hygral forces, and $\{M_{CMtX}\}$ are the hygral moments.

The finite element analysis module accepts the through-the-thickness composite properties that are given by Equation (1) for each node and performs the analysis at each load increment. After an incremental finite element analysis, the computed generalized nodal force resultants and deformations are supplied to the ICAN module that evaluates the nature and amount of local damage, if any,

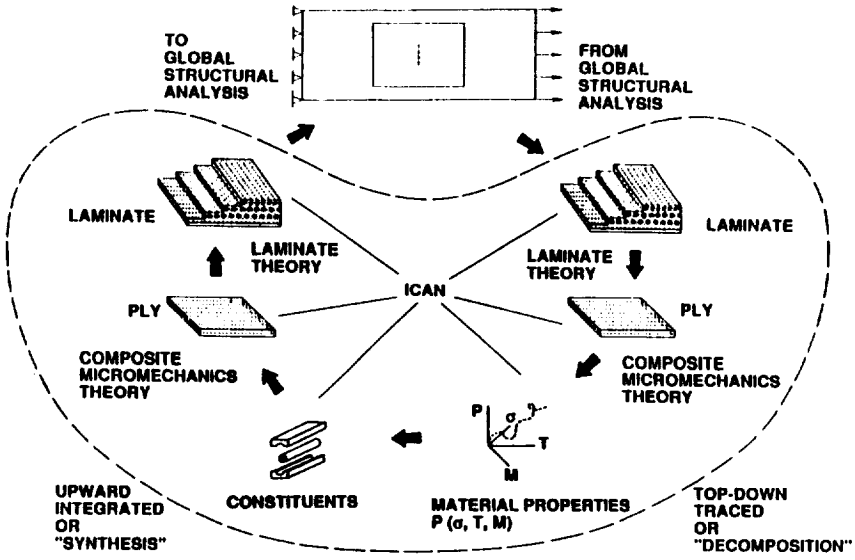

Figure 1. *CODSTRAN simulation cycle.*

in the plies of the composite laminate. Individual ply failure modes are assessed by ICAN using failure criteria associated with the negative and positive limits of the six ply-stress components in the material directions as follows:

$$S_{f11C} < \sigma_{f11} < S_{f11T} \tag{2}$$

$$S_{f22C} < \sigma_{f22} < S_{f22T} \tag{3}$$

$$S_{f33C} < \sigma_{f33} < S_{f33T} \tag{4}$$

$$S_{f12(-)} < \sigma_{f12} < S_{f12(+)} \tag{5}$$

$$S_{f23(-)} < \sigma_{f23} < S_{f23(+)} \tag{6}$$

$$S_{f13(-)} < \sigma_{f13} < S_{f13(+)} \tag{7}$$

In addition to the failure criteria based on the above stress limits, interply delamination due to relative rotation of the plies, and a modified distortion energy (MDE) failure criterion that takes into account combined stresses is considered. The MDE failure criterion is expressed as:

$$F = 1 - \left[\left(\frac{\sigma_{f11\alpha}}{S_{f11\alpha}}\right)^2 + \left(\frac{\sigma_{f22\beta}}{S_{f22\beta}}\right)^2 - K_{f12\alpha\beta}\frac{\sigma_{f11\alpha}}{S_{f11\alpha}}\frac{\sigma_{f22}}{S_{f22}} + \left(\frac{\sigma_{f12S}}{S_{f12S}}\right)^2\right] \tag{8}$$

where α and β indicate tensile or compressive stress, $S_{f11\alpha}$ is the local longitudinal strength in tension or compression, $S_{f22\alpha}$ is the transverse strength in tension or compression, and

$$K_{f12\alpha\beta} = \frac{(1 + 4\nu_{f12} - \nu_{f13})E_{f22} + (1 - \nu_{f23})E_{f11}}{[E_{f11}E_{f22}(2 + \nu_{f12} + \nu_{f13})(2 + \nu_{f21} + \nu_{f23})]^{1/2}} \tag{9}$$

The type of failure is assessed by comparison of the magnitudes of the squared terms in Equation (8). Depending on the dominant term in the MDE failure criterion, fiber failure or matrix failure is assigned. The generalized stress-strain relationships are revised locally according to the composite damage evaluated after each finite element analysis. The model is automatically updated with a new finite element mesh having reconstituted properties, and the structure is reanalyzed for further deformation and damage. If there is no damage after a load increment, the structure is considered to be in equilibrium and an additional load increment is applied leading to possible damage growth accumulation, or propagation. The CODSTRAN incremental loading procedure uses an accuracy criterion based on the allowable maximum number of damaged and fractured nodes within a simulation cycle during the application of a load increment. If too many nodes are damaged or fractured in a simulation cycle, incremental loads are reduced and the analysis is restarted from the previous equilibrium state. Otherwise, if there

is an acceptable amount of incremental damage, the incremental load is kept constant but the constitutive properties and the structural geometry are updated to account for the damage and deformations from the last simulation cycle.

When all modes of composite resistance fail at a node, that node is deleted and new detached nodes are created at the same point for the remaining adjacent finite elements. The number of new nodes created in place of a deleted node is equal to the number of elements that have connectivity to that deleted node. For laminated composite structures modeled via quadrilateral shell elements, if a deleted node were being shared by four elements, then four new nodes are required in place of the deleted node. When two adjacent nodes of a quadrilateral shell element are failed, that element is removed from the mesh.

After a valid simulation cycle in which composite structural degradation is simulated with or without the possible deletion of nodes and elements, the structure is reanalyzed for further damage and deformation. When there is no indication of further damage under a load, the structure is considered to be in equilibrium. Subsequently, another load increment is applied leading to possible damage growth, accumulation, or propagation. Analysis is stopped when global structural fracture is predicted.

Figure 2 shows a schematic of CODSTRAN damage tracking, expressed in terms of a load-displacement relationship. Point 1 represents the last equilibrium state before initial damage. When the structure is loaded by an additional load increment to point 2, ply failure criteria indicate damage initiation. At this stage

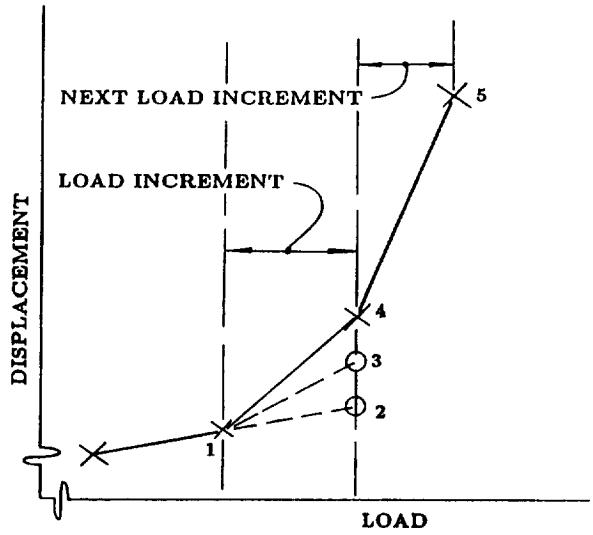

Figure 2. *CODSTRAN damage tracking—representative points: 1. Equilibrium—no damage. 2. Initial damage: degrade properties. 3. Damage accumulation: more degradation. 4. Damage stabilization: no additional damage. 5. Damage propagation.*

CODSTRAN degrades the composite properties affected by the damage, reconstitutes a new computational model with updated finite element mesh and material properties, and reanalyzes the structure under the same load increment to reach point 3. However, at point 3, composite ply failure criteria indicate additional damage. Accordingly, structural properties are further degraded and analysis is repeated under the same load increment to reach point 4. There is no further damage at point 4, because the structure is now in equilibrium with the external loads. Subsequently, another load increment is applied leading to point 5 with possible damage growth and progression. Nodal fracture is predicted when major principal failure criteria are met for all composite plies as well as through the thickness of aluminum panel at a node. Fracture zones are created by the fracturing of several adjacent nodes. Typically, an angle-plied composite structure experiences global fracture by the coalescence of multiple fracture zones. In the computational simulation cases presented in this paper analysis is continued through the stage of fracture propagation that breaks the specimen into two pieces.

COMPOSITE PATCH REPAIRED ALUMINUM

An aluminum tensile specimen of length L = 305 mm (12 in.), width W = 76 mm (3.0 in), and thickness t = 3 mm (0.12 in.) is considered. The specimen has an initial defect/crack at its center. The central defect is oriented transverse to the tensile load direction. Defects of length 2.54, 7.62, 12.7 mm (0.1, 0.3, and 0.5 in.) are considered. The composite patch measures 50.8 mm (2.0 in.) wide, 76.2 mm (3.0 in.) long, and is bonded to the surface of the aluminum tensile specimen, centered at the defect. Figure 3 shows a schematic of the patched aluminum tensile specimen. The patch laminate structure consists of twelve 0.132 mm (0.00521 in.) thick plies resulting in a composite patch thickness of 1.59 mm (0.063 in.). The composite system is made of AS-4 graphite fibers in a high-modulus, high strength (HMHS) epoxy matrix. The fiber and matrix constituent properties, as well as properties of the aluminum, are obtained from a databank of material properties resident in CODSTRAN [2]. The corresponding properties are given in Tables 1, 2, and 3. The HMHS matrix properties are representative of the 3501-6 resin. The fiber volume ratio is 0.60 and the void volume ratio is 2 percent. The cure temperature for the composite patch is 96.1°C (205°F) and the loading temperature is 21°C (70°F). The adhesive bond between the patch and the aluminum panel is assumed to have the same properties as the HMHS epoxy matrix.

The aluminum panel was subdivided into twelve 0.254 mm (0.01 in.) uniform layers to allow the simulation of damage progression across the aluminum thickness. At locations where composite patch was applied, quadrilateral plate finite elements included both the composite laminate and aluminum layers. The reference points of nodes with combined composite/aluminum were shifted in the out-of-plane z coordinate direction to represent the spatial configuration of the patch repaired aluminum accurately. The defect was simulated by prescribing local failures in the aluminum prior to the application of the load. The finite element size

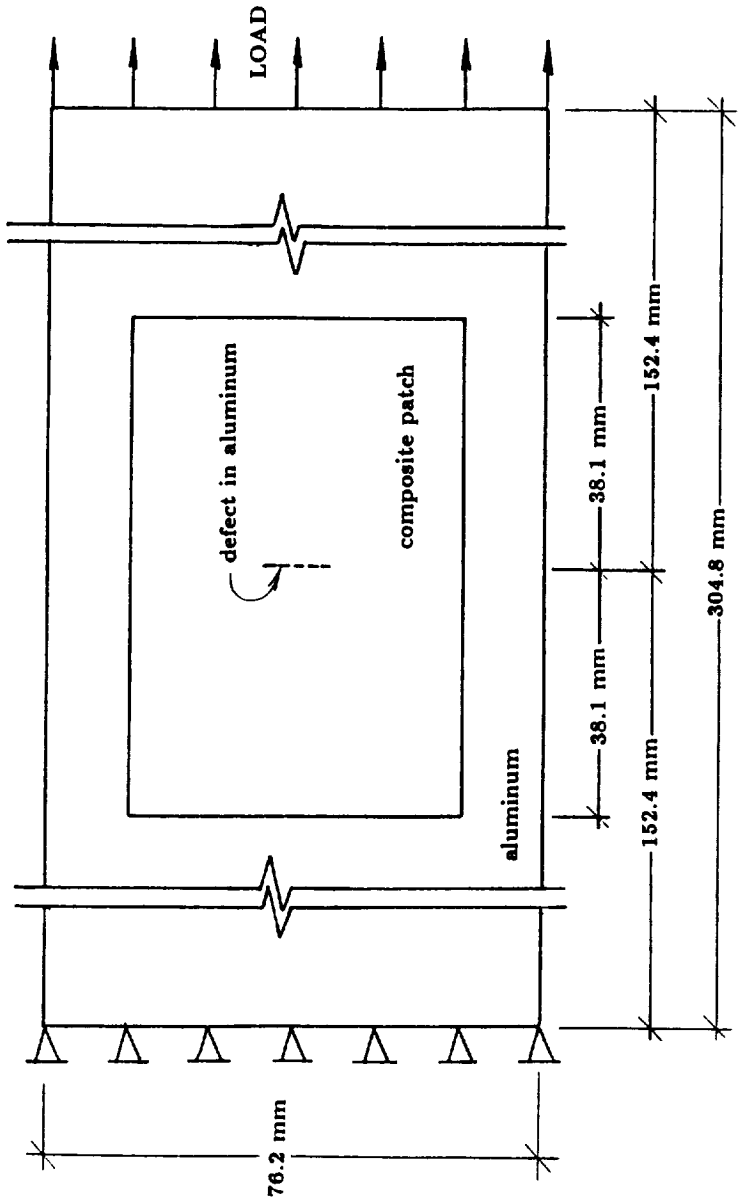

Figure 3. *Composite patch repaired aluminum. Aluminum thickness = 3.05 mm (0.12 in.); composite patch thickness = 1.6 mm (0.063 in.) defect in aluminum is transverse to tensile load, defect lengths considered: 2.54, 7.62, and 12.7 mm (0.1, 0.3, and 0.5 in.).*

Table 1. AS-4 Graphite fiber properties.

Number of fibers per end = 10,000
Fiber diameter = 0.00762 mm (0.300 E − 3 in.)
Fiber density = 1.74 E + 3 Kg/m^3 (0.063 lb/in^3)
Longitudinal normal modulus = 227 GPa (32.90 E + 6 psi)
Transverse normal modulus = 13.7 GPa (1.99 E + 6 psi)
Poisson's ratio (ν_{12}) = 0.20
Poisson's ratio (ν_{23}) = 0.25
Shear modulus (G_{12}) = 13.8 GPa (2.00 E + 6 psi)
Shear modulus (G_{23}) = 6.90 GPa (1.00 E + 6 psi
Longitudinal thermal expansion coefficient = 1.0 E − 6/°C (−0.55 E − 6/°F)
Transverse thermal expansion coefficient = 1.0 E − 6/°C (−0.56 E − 6/°F)
Longitudinal heat conductivity = 43.4 J-m/hr/m^2/°C (580 BTU-in/hr/in^2/°F)
Transverse heat conductivity = 4.34 J-m/hr/m^2/°C (58 BTU-in/hr/in^2/°F)
Heat capacity = 712 J/Kg/°C (0.17 BTU/lb/°F)
Tensile strength = 3,723 MPa (540 ksi)
Compressive strength = 3.351 MPa (486 ksi)

Table 2. HMHS Epoxy matrix properties.

Matrix density = 1.26 E + 3 Kg/m^3 (0.457 lb/in^3)
Normal modulus = 4.27 GPa (620 ksi)
Poisson's ratio = 0.34
Coefficient of thermal expansion = 0.72 E − 4/°C (0.4 E − 4/°F)
Heat conductivity = 0.0935 J-m/hr/m^2/°C (1.25 BTU-in/hr/in^2/°F)
Heat capacity = 1.05 E + 3 J/Kg/°C (0.25 BTU/lb/°F)
Tensile strength = 84.8 MPa (12.3 ksi)
Compressive strength = 423 MPa (61.3 ksi)
Shear strength = 148 MPa (21.4 ksi)
Allowable tensile strain = 0.02
Allowable compressive strain = 0.05
Allowable shear strain = 0.04
Allowable torsional strain = 0.04
Void conductivity = 0.0168 J-m/hr/m^2/°C (0.225 BTU-in/hr/in^2/°F)
Glass transition temperature = 216°C (420°F)

Table 3. ALT6 Aluminum properties.

Density = 1.22 E + 3 KG/m^3 (0.043 lb/in^3)
Normal modulus = 68.95 GPa (10,000 ksi)
Poisson's ratio = 0.33
Coefficient of thermal expansion = 2.32 E − 5/°C (1.29 E − 5/°F)
Heat conductivity = 7.78 J-m/hr/m^2/°C (104 BTU-in/hr/in^2/°F)
Heat capacity = 963 J/Kg/°C (0.23 BUT/lb/°F)
Tensile strength = 358 MPa (52 ksi)
Compressive strength = 358 MPa (52 ksi)
Shear strength = 179 MPa (26 ksi)
Allowable tensile strain = 0.0052
Allowable compressive strain = 0.0052
Allowable shear strain = 0.0905
Allowable torsional strain = 0.00905
Void conductivity = 0.0168 J-m/hr/m^2/°C (0.225 BTU-in/hr/in^2/°F)
Glass transition temperature = 582°C (1080°F)

at the vicinity of the defect was 0.1 in. Computed results are presented up to global fracture for each simulated case.

In general, overall structural damage may include individual ply damage and also through-the-thickness fracture of the composite laminate. CODSTRAN is able to simulate varied and complex composite damage mechanisms via evaluation of the individual ply failure modes and associated degradation of laminate properties. The type of damage growth and the sequence of damage progression depend on the composite structure, loading, material properties, and hygrothermal conditions. A scalar damage variable, derived from the total volume of the composite material affected by the various damage mechanisms is also evaluated as an indicator of the level of overall damage induced by loading. This scalar damage variable is useful for assessing the overall degradation of a given structure under a prescribed loading condition. The rate of increase in the overall damage during composite degradation may be used as a measure of structural propensity for fracture. Computation of the overall damage variable has no interactive feedback on the detailed simulation of composite degradation. The procedure by which the overall damage variable is computed is given in Reference [5].

Figure 4 shows damage progression for the aluminum specimen, with three different defect sizes and without a patch repair. As expected, the fracture load decreases with increasing defect size. Figure 5 shows damage progression for patch repaired specimens that have 2.54 mm (0.1 in.) defects. Four different patch laminate configurations are investigated. The best performances are given by the $[0/90/\pm 45/90/0]_S$ or $[\pm 45/90_2 0_2]_S$ configuration and the worst performance is by the $[90/0]_{3S}$ cross-ply laminate. Figure 6 shows the damage progression for $[\pm 45/90_2/0_2]_S$ patch with three different defect sizes. Figure 7 indicates the

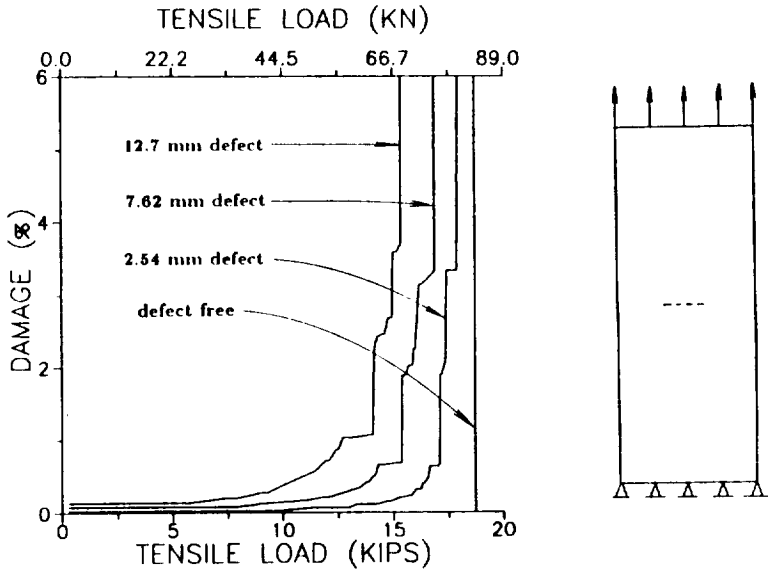

Figure 4. *Damage progression for aluminum specimen without patch.*

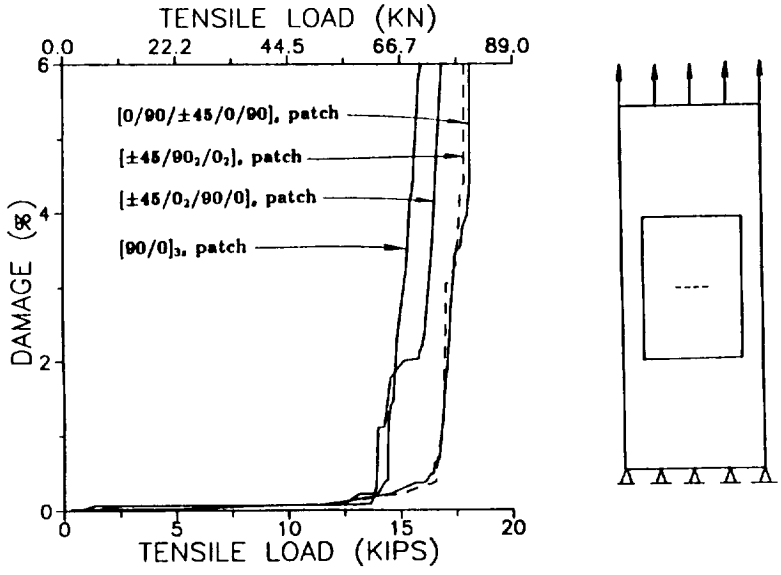

Figure 5. *Patch laminate configuration effect on damage progression. Defect length = 12.7 mm (0.5 in.), graphite/epoxy patch.*

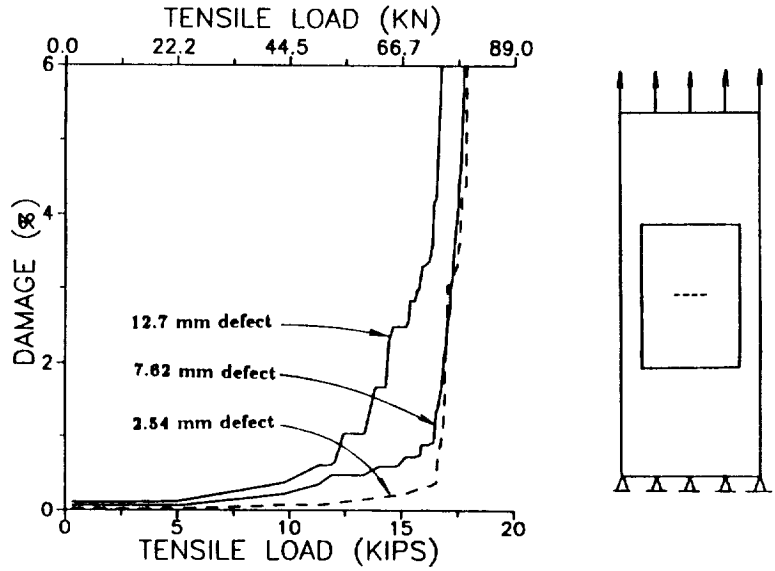

Figure 6. *Defect size effect on damage progression. Graphite/epoxy* $[\pm 45/90_2/0_2]_S$ *patch.*

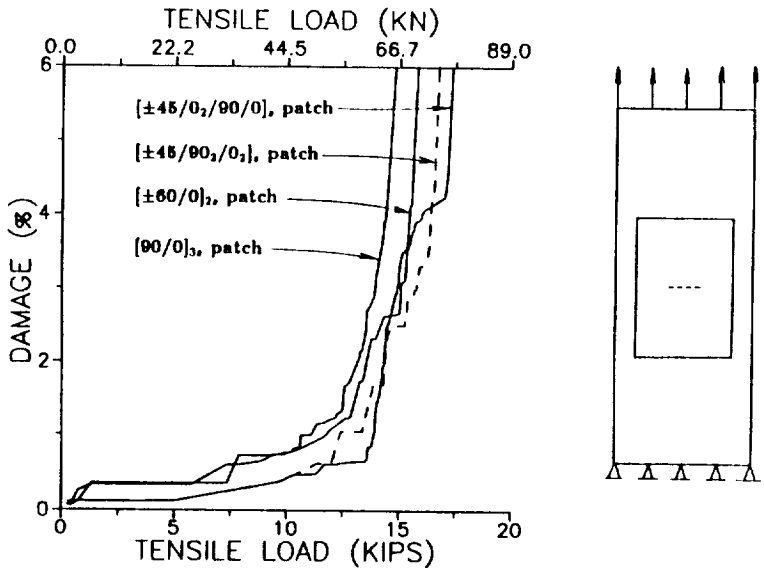

Figure 7. *Patch laminate configuration effect on damage progression. Defect length = 12.7 mm (0.5 in.), graphite/epoxy patch.*

differences among different patch laminates for damage progression from a 12.7 mm (0.5 in.) defect.

Damage progression characteristics have the following general features:

1. Damage initiation is by matrix cracking due to transverse tension in the 90° plies of the composite patch adjacent to the defect in aluminum.
2. Damage growth is by further degradation of the patch with fiber fractures as well as new matrix failures in the angle plies.
3. In spite of composite damage growth, the patch is effective as a crack arrestor, inhibiting growth of the initial defect in aluminum.
4. Damage/fracture propagation characteristics depend on the patch laminate configuration.

Figure 8 shows damage energy release rates for $[\pm 45/90_2/0_2]_s$ and $[90/0]_{3s}$ patches. The $[90/0]_{3s}$ cross-ply patch shows a very low resistance to initial damage growth from the 12.7 mm (0.5 in.) aluminum defect. On the other hand, the $[\pm 45/90_2/0_2]_s$ patch shows a very high initial resistance to damage growth. The directions of damage growth and progression for the two patches are distinctly different as seen in Figure 9.

Figure 10 shows the effect of combined shear and tension loading on damage progression for a $[\pm 45/90_2/0_2]_s$ patch. Very low levels of shear loading do not have a significant effect. However, when the magnitude of the shear loading becomes comparable to the tensile loading, the shear load becomes a very signifi-

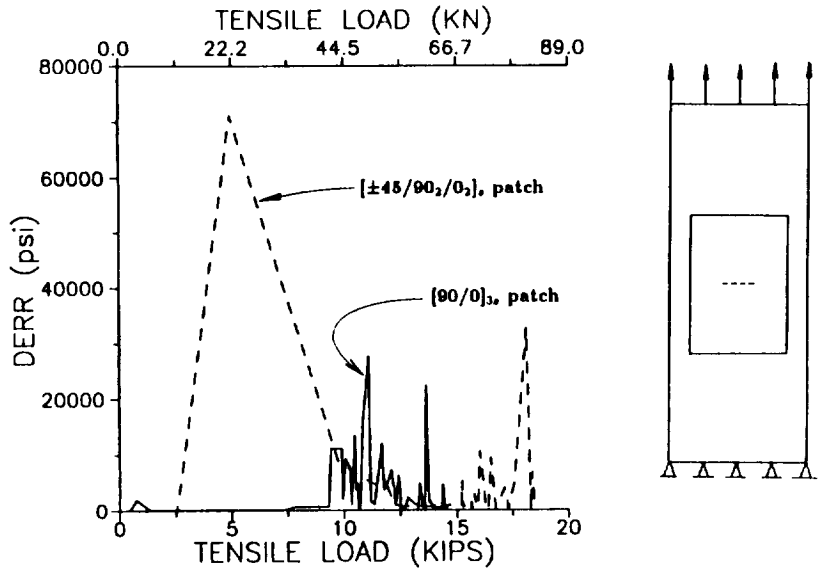

Figure 8. *Laminate configuration effect on damage energy release rates. Defect length = 12.7 mm (0.5 in.), graphite/epoxy patch.*

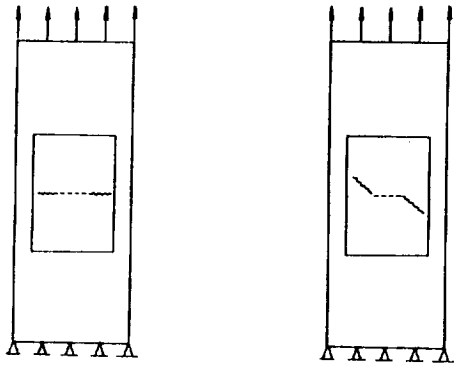

Figure 9. *Effect of patch laminate on damage/fracture orientation.*

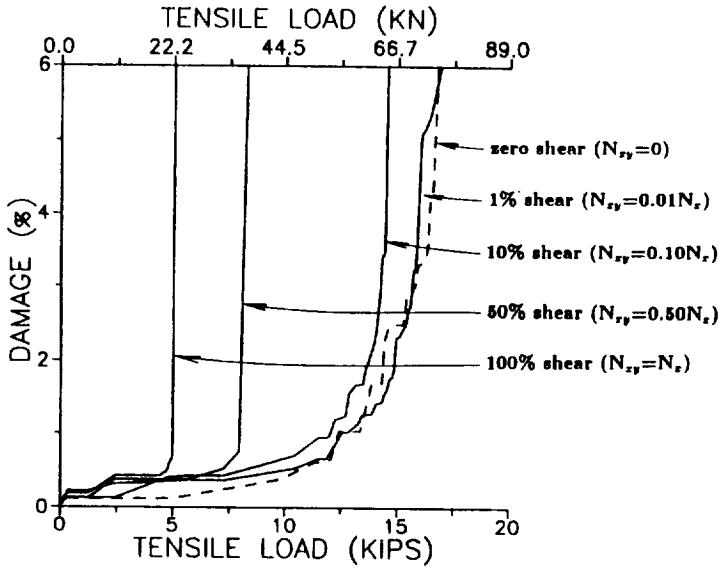

Figure 10. *Damage progression under combined loading. Defect length = 12.7 mm (0.5 in., graphite/epoxy* $[\pm 45/90_2/0_2]_S$ *patch.*

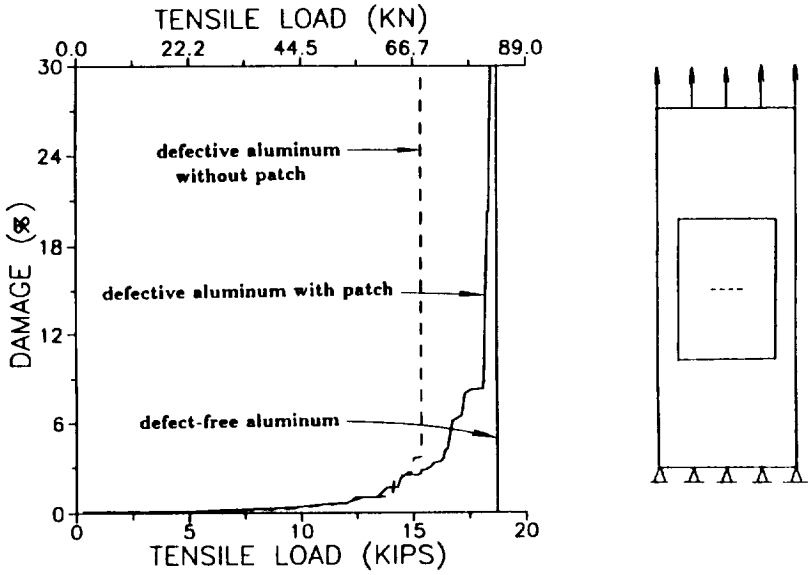

Figure 11. *Strength recovery due to patch repair. Defect length = 12.7 mm (0.5 in.). Graphite/epoxy* $[\pm 45/90_2/0_2]_S$ patch.

cant factor for damage propagation. Also, ultimate fracture propagation becomes more sudden when the shear load is larger.

Figure 11 shows the strength recovery due to a $[\pm 45/90_2/0_2]_S$ patch repair on the original aluminum specimen with 12.7 mm (0.5 in.) defect. The full strength of defect-free aluminum is practically regained by the patch repair. Additionally, the composite patch repaired specimen is more damage tolerant compared to the original defect-free aluminum. The demonstrated quantification of defect and damage tolerance for a given patch repair is fundamental in the process of identifying the optimal laminate configuration for each application.

SUMMARY OF RESULTS AND GENERALIZATION

A computational simulation methodology has been demonstrated for the evaluation of progressive fracture and durability of composite patch repaired aluminum panels. The relative effectiveness of various composite patches with different layups were assessed. Damage progression characteristics were identified as function of the patch laminate configuration. Simulations indicated fiber composite patches experienced damage initiation adjacent to the aluminum defect during service loading. Nevertheless, damage tolerance is increased significantly due to composite patch repair. DERR levels help identify and distinguish the levels of structural resistance against damage progression for different patches. It is shown that high levels of shear loading combined with tension may degrade composite

patch repairs prematurely unless properly designed for combined loading service. Tensile strength recovery is excellent for well designed composite patch repaired aluminum panels.

The presented computational simulation method is suitable for the design and continued in-service evaluation of composite patch repaired aluminum tension panels. The effectiveness of fiber composite patches with different constituents and ply layups can be evaluated under tension, compression, shear, and combined loading. The basic procedure is to simulate a computational model of the patched aluminum structure subjected to the expected loading environments. Computational simulation may be used to address design questions as follows:

1. Evaluation of structural resistance to fracture propagation: Computational simulation characterizes the evolution of damage and fracture that would be caused due to overloading by the type of load the composite patch repaired structure is designed to carry. Once a structural damage level is defined, resistance to damage propagation is evaluated by monitoring damage growth and progression from the damaged state to ultimate fracture. Significant parameters that quantify damage stability and fracture progression characteristics are the rate of damage increase with incremental loading, damage energy release rate, and the rate of structural displacements with loading. Identification of damage initiation/progression mechanisms and the sequence of progressive fracture modes convey serviceable information to help with critical decisions in the structural design process. Determination of design allowables based on damage tolerance requirements is an inherent use of the computational simulation results. Simulation of progressive fracture from defects allows setting of quality acceptance criteria for composite patch repaired structures as appropriate for each functional requirement. Detailed information on specific damage tolerance characteristics help establish criteria for the removal and replacement of a composite patch repair for due cause.
2. Determination of sensitive parameters affecting composite patched structural fracture: Computational simulation indicates the damage initiation, growth, and progression modes in terms of a damage index that is printed out for the degraded composite plies and metallic layers at each damaged node. In turn, the damage index points out the fundamental physical parameters that characterize the degradation. For instance, if the damage index shows composite ply transverse tensile failure, the fundamental physical parameters are matrix tensile strength, fiber volume ratio, matrix modulus, and fiber transverse modulus; of which the most significant parameter is the matrix tensile strength [2]. In addition to the significant parameters identified by the ply damage index, sensitivity to hygrothermal parameters may be obtained by simulating the patch repaired structure at different temperatures and moisture contents. Similarly, sensitivity to residual stresses may be assessed by simulating the composite patch cured at different stress-free temperatures. Identification of important parameters that significantly affect structural performance for each design case allows optimization of the composite patch for best structural durability. Sensitive parameters may be fiber and matrix

strength, stiffness, laminate configuration, cure temperature, and environmental factors.

CONCLUSIONS

1. Computational simulation, with the use of established composite mechanics and finite element modules, can be used to predict the influence of an existing defect as well as loading, on the safety and durability of a composite patch repaired aluminum panel.
2. CODSTRAN adequately tracks the damage growth and subsequent propagation to fracture for a patch repaired aluminum specimen with an initial defect.
3. Damage initiation, growth, and accumulation stages involve matrix cracking as well as fiber fractures in the composite patch area that is contiguous to the initial defect in aluminum.
4. The demonstrated procedure is flexible and applicable to all types of constituent materials, structural geometry, and loading. Homogeneous materials as well as composites can be simulated.
5. Fracture toughness parameters such as the structural fracture load and damage progression characteristics are identifiable for any composite/metallic structure with any defect by the demonstrated method.
6. Computational simulation by CODSTRAN represents a new global approach to progressive damage and fracture assessment for any structure.

REFERENCES

1. Chamis, C. C., and G. T. Smith. 1978. "Composite Durability Structural Analysis," NASA TM-79070.
2. Murthy, P. L. N., and C. C. Chamis. 1986. *Integrated Composite Analyzer (ICAN): Users and Programmers Manual*, NASA Technical Paper 2515, March.
3. Nakazawa, S., J. B. Dias, and M. S. Spiegel. 1987. *MHOST Users' Manual*, Prepared for NASA Lewis Research Center by MARC Analysis Research Corp., April.
4. Minnetyan, L., C. C. Chamis, and P. L. N. Murthy. 1992. "Structural Behavior of Composites with Progressive Fracture," *Journal of Reinforced Plastics and Composites*, 11(4):413-442.
5. Minnetyan, L., P. L. N. Murthy, and C. C. Chamis. 1990. "Composite Structure Global Fracture Toughness via Computational Simulation," *Computers & Structures*, 37(2):175-180. November.
6. Minnetyan, L., P. L. N. Murthy, and C. C. Chamis. 1992. "Progressive Fracture in Composites Subjected to Hygrothermal Environment," *International Journal of Damage Mechanics*, 1(1):60-79.
7. Minnetyan, L., C. C. Chamis, and P. L. N. Murthy. 1992. "Structural Durability of a Composite Pressure Vessel," *Journal of Reinforced Plastics and Composites*, 11(11):1251-1269.
8. Minnetyan, L., and C. C. Chamis. 1995. 1995. "Pressure Vessel Fracture Simulation," Presented at the ASTM 25th National Symposium on Fracture Mechanics, Lehigh University, Bethlehem, Pennsylvania, June 28-July 1, 1993, Published in ASTM STP 1220, *Fracture Mechanics: 25th Volume*, August. pp. 671-684.
9. Minnetyan, L., J. M. Rivers, C. C. Chamis, and P. L. N. Murthy. 1995. "Discontinuously Stiffened Composite Panel under Compressive Loading," *Journal of Reinforced Plastics and Composites*, 14(1):85-98.